

Lateral and normal forces between patterned substrates induced by nematic fluctuations

F. Karimi Pour Haddadan* and S. Dietrich

*Max-Planck-Institut für Metallforschung,
Heisenbergstr. 3, D-70569 Stuttgart, Germany,*
and

*Institut für Theoretische und Angewandte Physik,
Universität Stuttgart, Pfaffenwaldring 57,
D-70569 Stuttgart, Germany*

(Dated: September 21, 2018)

We consider a nematic liquid crystal confined by two parallel flat substrates whose anchoring conditions vary periodically in one lateral direction. Within the Gaussian approximation, we study the effective forces between the patterned substrates induced by the thermal fluctuations of the nematic director. The shear force oscillates as function of the lateral shift between the patterns on the lower and the upper substrates. We compare the strength of this fluctuation-induced lateral force with the lateral van der Waals force arising from chemically structured adsorbed monolayers. The fluctuation-induced force in normal direction is either repulsive or attractive, depending on the model parameters.

PACS numbers: 61.30.Dk, 61.30.Hn

I. INTRODUCTION

Liquid crystals are characterized by large thermal fluctuations in their local orientational order arising from collective alignment of the long axis of their constituent molecules [1]. Due to such soft anisotropy, liquid crystals tend to respond easily to external forces. Confining geometries such as thin films, on which most applications of liquid crystals are based, change the fluctuation spectrum. This can cause not only structural changes [2, 3] but also leads to fluctuation-induced effective forces between the substrates [4], also known as thermodynamic Casimir effect. In correlated fluids such as liquid crystals this Casimir force exhibits a universal power-law decay as a function of the separation between the substrates [5]. However, this behavior is modified in the presence of other characteristic scales in the system [6, 7, 8]. In the case that the substrates are laterally modulated, discrete lateral modes of thermal fluctuations are also excited. Under such conditions, in addition to the forces acting perpendicularly to the substrates, effective lateral forces arise [9, 10] with potentially interesting technological applications. We study the influence of anchoring conditions, which vary periodically in one lateral direction, on the fluctuations of a uniformly ordered nematic liquid crystal. Obviously, the periodicity ζ of the substrate pattern gives rise to an oscillatory behavior for the lateral force as a function of the lateral shift δ between the substrates. For small inhomogeneities the

lateral force is proportional to $\sin(2\pi\delta/\zeta)$. (The analysis of nonperiodic patterns would provide an understanding of nematic phases exposed to chemically disordered substrates.) The present study actually extends our previous work [11] where we considered the case in which only one of two confining substrates exhibits a chemical pattern so that there are no lateral forces. Here, in addition to the fluctuation-induced lateral forces, we calculate the lateral force between the patterned substrates across the vacuum, i.e., the background van der Waals force acting parallel to the substrates. This background force is generated by the necessary chemical modulations providing the laterally varying anchoring strengths.

In Sec. II our model and the theoretical formalism are specified. In Sec. III A the fluctuation-induced lateral force is obtained. In Sec. III B we calculate the lateral van der Waals force between the patterned substrates. The results for the fluctuation-induced normal force are presented in Sec. IV and finally Sec. V summarizes our results.

II. SYSTEM AND FORMALISM

We consider a nematic liquid crystal confined by two flat but chemically patterned substrates at a separation d . The patterns on the both substrates consist of the same periodic stripes of anchoring energies per area W_a and W_b along the x direction but shifted relative to each other by the length δ (see Fig. 1). The substrates are translationally invariant in the y direction. The stripes are considered to vary with respect to the strength of homeotropic anchoring so that the mean orientation of the director \mathbf{n} is spatially homogeneous but the thermal fluctuations vary laterally giving rise to effective lateral

*Present address: Institute for Studies in Theoretical Physics and Mathematics (IPM), School of Physics, PO Box 19395-5531, Tehran, Iran

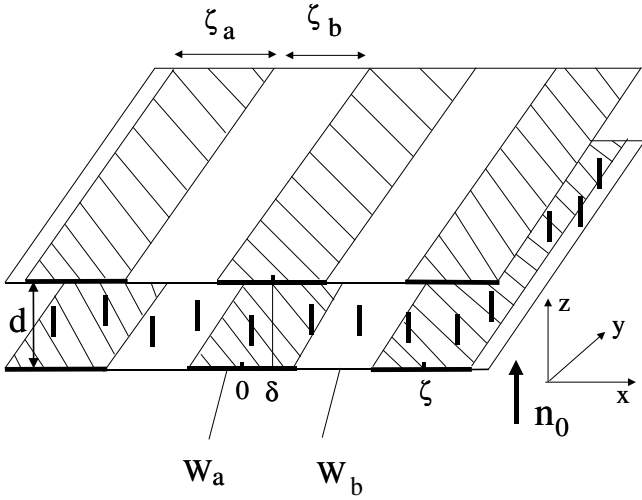


FIG. 1: The geometry of the nematic cell with patterned substrates. The patterns on both substrates are the same but shifted relative to each other. The patterns consist of periodic stripes of anchoring energies per area W_a and W_b with the widths ζ_a and ζ_b , respectively. The wavelength of the periodicity is denoted as $\zeta = \zeta_a + \zeta_b$ and the lateral shift between the origins of the patterns on the top and the bottom substrate is denoted by δ . Anchoring at both boundaries is homeotropic everywhere so that the thermal average of the director field $\mathbf{n}_0 = \hat{\mathbf{z}}$ is spatially homogeneous.

forces. Based on the bulk structural Frank free energy [1] given by

$$F_b[\mathbf{n}] = \frac{1}{2} \int_V d^3x \left[K_1 (\nabla \cdot \mathbf{n})^2 + K_2 (\mathbf{n} \cdot \nabla \times \mathbf{n})^2 + K_3 (\mathbf{n} \times \nabla \times \mathbf{n})^2 \right], \quad (1)$$

where V is the nematic volume, K_1 , K_2 , and K_3 are the splay, the twist, and the bend elastic constants, respectively, the free energy of Gaussian fluctuations in the one-constant approximation reads

$$F_b[\nu_1, \nu_2] = \sum_{i=1}^2 \frac{K}{2} \int_V d^3x [\nabla \nu_i(\mathbf{x}, z)]^2, \quad (2)$$

where ν_i , $i = 1, 2$, is either of the two independent components of the fluctuating part $\delta \boldsymbol{\nu} = \mathbf{n} - \mathbf{n}_0$ of the director \mathbf{n} , $K = K_1 = K_2 = K_3$ is the effective elastic constant, and $\mathbf{x} = (x, y)$ are the lateral components of the Cartesian coordinates $\mathbf{r} = (\mathbf{x}, z)$.

To describe the interaction of the liquid crystal and the substrates, we employ the Rapini-Papoular surface free energy given by

$$F_s[\mathbf{n}] = -\frac{1}{2} \int_S d^2x W^{z=0}(\mathbf{x}) (\mathbf{n} \cdot \hat{\mathbf{z}})^2 - \frac{1}{2} \int_S d^2x W^{z=d}(\mathbf{x}) (\mathbf{n} \cdot \hat{\mathbf{z}})^2 = F_s^{z=0} + F_s^{z=d} \quad (3)$$

where W is the anchoring energy per area S and $\hat{\mathbf{z}}$ is the unit vector in z -direction. Here $W^{z=0}(x) = W_a a(x) +$

$W_b [1 - a(x)]$ at the lower substrate located at $z = 0$ and $W^{z=d}(x) = W_a b(x) + W_b [1 - b(x)]$ at the upper substrate located at $z = d$ where

$$a(x) = \sum_{k=-\infty}^{\infty} \Theta\left(x - k\zeta + \frac{\zeta}{4}\right) \Theta\left(k\zeta + \frac{\zeta}{4} - x\right) \quad (4)$$

and

$$b(x) = a(x + \delta) \quad (5)$$

describe the stripe modulations at the lower and the upper substrates, respectively, $\Theta(x)$ is the Heaviside step function, and ζ is the periodicity. The stripes have the same width $\zeta_a = \zeta_b = \zeta/2$ and are separated by sharp chemical steps. The functions $a(x)$ and $b(x)$ equal one at the regions characterized by W_a and zero elsewhere at the lower and the upper substrates, respectively. Thus the surface free energy of the Gaussian fluctuations given by $F_s[\nu_1, \nu_2] = F_s[\nu_1] + F_s[\nu_2]$ reads

$$F_s^{z=0}[\nu] = \frac{1}{2} \left[W_a \int_S d^2x [\nu(\mathbf{x}, z=0)]^2 a(x) + W_b \int_S d^2x [\nu(\mathbf{x}, z=0)]^2 [1 - a(x)] \right] \quad (6)$$

at the lower substrate and

$$F_s^{z=d}[\nu] = \frac{1}{2} \left[W_a \int_S d^2x [\nu(\mathbf{x}, z=d)]^2 b(x) + W_b \int_S d^2x [\nu(\mathbf{x}, z=d)]^2 [1 - b(x)] \right] \quad (7)$$

at the upper substrate.

Minimization of total free energy $F = F_b[\nu_1, \nu_2] + F_s^{z=0}[\nu_1, \nu_2] + F_s^{z=d}[\nu_1, \nu_2]$ leads to two boundary conditions:

$$-K \partial_z \nu(\mathbf{x}, z) + W_a \nu(\mathbf{x}, z) a(x) + W_b \nu(\mathbf{x}, z) [1 - a(x)] = 0, \quad z = 0, \quad (8a)$$

$$K \partial_z \nu(\mathbf{x}, z) + W_a \nu(\mathbf{x}, z) b(x) + W_b \nu(\mathbf{x}, z) [1 - b(x)] = 0, \quad z = d, \quad (8b)$$

where ν is either ν_1 or ν_2 .

A. Path integral technique

The normalized [see, c.f., after Eq. (9)] partition function Z of the fluctuating fields ν_i , $i = 1, 2$, subject to the boundary conditions given by Eqs. (8a) and (8b) can be calculated within the path integral approach (see Ref. [11] and references therein). The boundary conditions act as constraints which can be implemented by delta functions. They, in turn, can be written as integral representations by introducing two auxiliary fields localized at $z = 0$ and $z = d$, respectively [12, 13]. After performing the corresponding Gaussian integrals over

ν_i , $i = 1, 2$, the path integral reduces to a Gaussian functional integral over the auxiliary fields with a matrix kernel M , so that obtaining the result for Z reduces

to calculating $(\det M)^{-1/2}$. For the geometry considered here, the matrix M is found to have the following matrix elements $M_{\alpha,\beta}$, $\alpha, \beta = 1, 2$:

$$\begin{aligned}
M_{11}(\mathbf{x}, \mathbf{x}') &= \left\{ \left[1 + \frac{\lambda_b - \lambda_a}{\lambda_a} a(x) \right] \left[1 + \frac{\lambda_b - \lambda_a}{\lambda_a} a(x') \right] \right. \\
&\quad \left. + \frac{\lambda_b(\lambda_b - \lambda_a)}{\lambda_a} [a(x) - a(x')] \partial_z - \lambda_b^2 \partial_z^2 \right\} G(\mathbf{x} - \mathbf{x}', z - z') \Big|_{z=z'=0}, \\
M_{12}(\mathbf{x}, \mathbf{x}') &= \left[1 + \frac{\lambda_b - \lambda_a}{\lambda_a} [a(x') + b(x)] - 2\lambda_b \partial_{z'} - \frac{\lambda_b(\lambda_b - \lambda_a)}{\lambda_a} [a(x') + b(x)] \partial_{z'} \right. \\
&\quad \left. + \left(\frac{\lambda_b - \lambda_a}{\lambda_a} \right)^2 a(x') b(x) + \lambda_b^2 \partial_{z'}^2 \right] G(\mathbf{x} - \mathbf{x}', z - z') \Big|_{z=d, z'=0}, \\
M_{21}(\mathbf{x}, \mathbf{x}') &= \left[1 + \frac{\lambda_b - \lambda_a}{\lambda_a} [a(x) + b(x')] - 2\lambda_b \partial_z - \frac{\lambda_b(\lambda_b - \lambda_a)}{\lambda_a} [a(x) + b(x')] \partial_z \right. \\
&\quad \left. + \left(\frac{\lambda_b - \lambda_a}{\lambda_a} \right)^2 a(x) b(x') + \lambda_b^2 \partial_z^2 \right] G(\mathbf{x} - \mathbf{x}', z - z') \Big|_{z'=d, z=0}, \\
M_{22}(\mathbf{x}, \mathbf{x}') &= \left\{ \left[1 + \frac{\lambda_b - \lambda_a}{\lambda_a} b(x) \right] \left[1 + \frac{\lambda_b - \lambda_a}{\lambda_a} b(x') \right] \right. \\
&\quad \left. + \frac{\lambda_b(\lambda_b - \lambda_a)}{\lambda_a} [b(x') - b(x)] \partial_z - \lambda_b^2 \partial_z^2 \right\} G(\mathbf{x} - \mathbf{x}', z - z') \Big|_{z=z'=d},
\end{aligned} \tag{9}$$

where $\lambda_{a(b)} = K/W_{a(b)}$ is the so-called extrapolation length and $G(\mathbf{r}, \mathbf{r}') = k_B T / (4\pi K |\mathbf{r} - \mathbf{r}'|)$ is the two-point correlation function of the scalar field ν_i in the bulk with its statistical weight given by $Z_0^{-1} \exp \left\{ \frac{K}{2k_B T} \int_V d^3x \nu_i(\mathbf{x}, z) \nabla^2 \nu_i(\mathbf{x}, z) \right\}$ where the normalizing factor Z_0 is the bulk partition function and $k_B T$ is the thermal energy.

In terms of the partition function Z , the free energy is given by $F = -k_B T \ln Z = (k_B T/2) \ln \det M$. We note that normalizing Z by Z_0 amounts to subtracting the bulk free energy, so that the free energy F includes only the surface free energy and the finite-size contribution. The surface free energy depends neither on d nor on δ , so the fluctuation-induced force $\mathcal{F} = -\partial F$ reads

$$\mathcal{F} = -\frac{k_B T}{2} \text{Tr} (M^{-1} \partial M), \tag{10}$$

where ∂ is either ∂_δ or ∂_d corresponding to lateral or normal displacements giving rise to lateral or normal forces, respectively.

B. Periodic modulation

The matrix kernel M is a functional of the patterning function $a(x)$ on the substrates and therefore calculation of the inverse of M is nontrivial. However, in systems with in-plane symmetries one may proceed by a lateral Fourier transformation with respect

to the lateral coordinates $\mathbf{x} = (x, y)$. In Ref. [14], it is shown how the electrodynamic Casimir force can be calculated for a periodically modulated substrate (see also Refs. [11, 15]). In this reference, the lateral periodicity is used to transform the matrix M to a block-diagonal form in Fourier space (\mathbf{p}, \mathbf{q}) in which $M(\mathbf{p}, \mathbf{q}) = \iint d^2x d^2x' M(\mathbf{x}, \mathbf{x}') e^{i\mathbf{p}\cdot\mathbf{x}} e^{i\mathbf{q}\cdot\mathbf{x}'}$. Similarly, also here the matrix elements of the block $M_j = (M_{j,kl})$ with $M_{j,kl}(p_y, q_y) = 2\pi \delta(p_y + q_y) B_{kl} \left(\frac{2\pi j}{L}, p_y \right)$, $j = 1, \dots, N = L/\zeta$, are given by

$$B_{kl} \left(\frac{2\pi j}{L}, p_y \right) = N_{m=k-l} \left(\frac{2\pi j}{L} + \frac{2\pi l}{\zeta}, p_y \right) \tag{11}$$

for $l, k \in \mathbb{Z}$, where L is the lateral extension of the system in the x direction and the N_m are (2×2) matrices providing the following decomposition of the matrix M :

$$\begin{aligned}
M(\mathbf{p}, \mathbf{q}) &= (2\pi)^2 \delta(p_y + q_y) \sum_{m=-\infty}^{\infty} N_m(p_x, p_y) \\
&\quad \times \delta \left(p_x + q_x + \frac{2\pi m}{\zeta} \right).
\end{aligned} \tag{12}$$

However, it is interesting to note that the matrix $M(\mathbf{x}, \mathbf{x}') = M(\mathbf{x} - \mathbf{x}', a(x), a(x'))$ can also be represented, using a more direct derivation than in Ref. [14], in a form in which M is diagonal [16]. In view of the discrete lateral periodicity along the x direction, it is suitable to

express x and x' as

$$x = n\zeta + s, \quad x' = n'\zeta + s', \quad (13)$$

with $n, n' \in \mathbb{Z}$ and $s, s' \in [0, \zeta)$. Since $a(x)$ is periodic with wavelength ζ it follows that $a(x) = a(s)$ and $x - x' = (n - n')\zeta + s - s'$ depends on n and n' only via the difference $n - n'$. This property and translational invariance along the y direction imply the Fourier decomposition

$$\begin{aligned} \hat{M}(p_x, p_y; s, s') &= \sum_{n, n' = -\infty}^{\infty} \int dy \int dy' \\ &\times M(n - n', y - y'; s, s') e^{-ip_x(n - n')\zeta} e^{-ip_y(y - y')} \end{aligned} \quad (14)$$

where $\hat{M}(p_x, p_y; s, s')$ is diagonal. Furthermore with $s, s' \in [0, \zeta)$ one can form

$$\begin{aligned} C_{kl}(p_x, p_y) &= \int_0^\zeta ds \int_0^\zeta ds' \\ &\times e^{2\pi i k s / \zeta} \hat{M}(p_x, p_y; s, s') e^{-2\pi i l s' / \zeta}. \end{aligned} \quad (15)$$

As expected, the different representations of M in terms of the matrices C or B (C is the Fourier transform of \hat{M} and B is the Fourier transform of $e^{-ip_x s} \hat{M} e^{ip_x s'}$) do not change the final result for the force [Eq. (10)] which is given by [14]

$$\begin{aligned} \mathcal{F} &= -\frac{k_B T S}{2\pi^2} \int_0^\infty dp_y \int_0^{2\pi/\zeta} dp_x \\ &\times \text{tr}(B^{-1}(p_x, p_y) \partial B(p_x, p_y)). \end{aligned} \quad (16)$$

Here tr denotes the partial trace with respect to the indices k, l of the infinite-dimensional matrix B (or C) and we have taken into account the contribution of both fluctuating components of the director field.

In the following we continue with the block-diagonal form of the matrix kernel M since in this representation the patterning functions a_k and b_k are somehow simpler than their counterparts in the diagonal form of M . Accordingly, the matrices N_m [Eq. (12)] are given by

$$\begin{aligned} N_m &= \begin{pmatrix} \phi_m^{aa}(0) & \phi_m^{ab}(d) \\ \phi_m^{ba}(d) & \phi_m^{bb}(0) \end{pmatrix} + \delta_{m,0} \begin{pmatrix} \frac{z_a^2}{2p} - \frac{\lambda_b^2 p}{2} & \frac{(1 - \lambda_b p)^2}{2p} e^{-pd} \\ \frac{(1 - \lambda_b p)^2}{2p} e^{-pd} & \frac{z_b^2}{2p} - \frac{\lambda_a^2 p}{2} \end{pmatrix} \\ &+ \frac{\lambda_b - \lambda_a}{2\lambda_a} \delta_{m,0} \begin{pmatrix} 0 & \left[a_0 \left(\frac{z_c}{p} - \lambda_b \right) + b_0 \left(\frac{z_a}{p} - \lambda_b \right) \right] e^{-pd} \\ \left[a_0 \left(\frac{z_b}{p} - \lambda_b \right) + b_0 \left(\frac{z_a}{p} - \lambda_b \right) \right] e^{-pd} & 0 \end{pmatrix} \end{aligned} \quad (17)$$

for m even, and

$$N_m = \frac{\lambda_b - \lambda_a}{2\lambda_a} \begin{pmatrix} a_m z_a \left(\frac{1}{p} + \frac{1}{p_m} \right) & a_m \left(\frac{z_b}{p} - \lambda_b \right) e^{-pd} + b_m \left(\frac{z_a}{p_m} - \lambda_b \right) e^{-p_m d} \\ b_m \left(\frac{z_a}{p} - \lambda_b \right) e^{-pd} + a_m \left(\frac{z_b}{p_m} - \lambda_b \right) e^{-p_m d} & b_m z_b \left(\frac{1}{p} + \frac{1}{p_m} \right) \end{pmatrix} \quad (18)$$

for m odd, with $z_{a(b)} = 1 + \frac{\lambda_b - \lambda_a}{\lambda_a} a_0(b_0)$, $z_{a(b)}^c = 1 + \frac{\lambda_b - \lambda_a}{2\lambda_a} a_0(b_0)$, $p_m = \sqrt{(p_x + 2\pi m/\zeta)^2 + p_y^2}$, $p = p_{m=0}$, $a_0 = b_0 = 1/2$, $a_{m=odd} = (-1)^{(|m|-1)/2} / (\pi|m|)$, $b_{m=odd} = e^{-2\pi i m \delta / \zeta} a_m$, and

$$\phi_m^{ab}(d) = \left(\frac{\lambda_b - \lambda_a}{\lambda_a} \right)^2 \sum_{k=-\infty}' a_{k-m} b_{-k} \frac{e^{-p_k d}}{2p_k}, \quad (19)$$

where the prime at the summation sign indicates that in the sum the terms with even k are excluded.

III. LATERAL FORCES

A. Fluctuation-induced shear forces

In the limit $d \gg \zeta$ we find that the contributions from the elements B_{kl} [Eqs. (11) and (12)] to the force decrease rapidly with increasing absolute values of k, l , so that the expression for the force [Eq. (16)] converges already at small orders of M with $k, l = -M, \dots, M$. Taking into account only the elements B_{kl} [Eq. (11)] for $k, l = -1, 0, 1$, the asymptotic behavior of the fluctuation-induced lateral force $\mathcal{F}_{\text{lat}} = -\partial_\delta F$ in the limit

$|\lambda_b - \lambda_a|/\lambda_a \ll 1$ is given by

$$\frac{\mathcal{F}_{\text{lat}}(d \gg \zeta)}{k_B T S} = \frac{8(\lambda_b - \lambda_a)^2}{\pi \zeta^3 \lambda_a^2} e^{-2\pi d/\zeta} \sin\left(\frac{2\pi\delta}{\zeta}\right) \times f(d/\zeta, \lambda_b/\zeta) + O\left(\left(\frac{\lambda_b - \lambda_a}{\lambda_a}\right)^3\right) \quad (20)$$

with the dimensionless function

$$f(u, v) = \frac{1}{(1 + 2\pi v)^2} \int_0^\infty dx e^{-ux} \times \frac{1 - \frac{1+2v(1-vx)x + (\frac{x}{2\pi})^2(1+4\pi v)}{(1-vx)^2} e^{2ux}}{1 - \left(\frac{1+vx}{1-vx}\right)^2 e^{2ux}}. \quad (21)$$

The lateral force oscillates as function of δ reflecting the underlying lateral periodic pattern and its magnitude decays exponentially as function of d/ζ , because $f(\infty, v) < \infty$.

For arbitrary values of d , we evaluate the force in Eq. (16) numerically. Although the matrix B [Eq. (11)] is infinite-dimensional, the value of the force saturates at some finite values for k, l . Our numerical results for the fluctuation-induced lateral force as function of the shift δ for arbitrary strength of the contrast $\lambda_b - \lambda_a$ are shown in Fig. 2. The lateral force acts against the increase of the lateral displacement δ in the interval $[0, \zeta/2)$ by being a restoring force and acts favorably with the increase of δ in the interval $(\zeta/2, \zeta]$ by being a pulling force. Therefore the force is antisymmetric with respect to $\delta/\zeta = 0.5$. Upon approaching the maximum misalignment, i.e., $\delta/\zeta = 0.5$, the restoring force vanishes. This implies that the interaction free energy $V_{\text{lat}}(\delta) = -\int_0^\delta \mathcal{F}_{\text{lat}}(\delta') d\delta'$ has its maximum at $\delta/\zeta = 0.5$ where the opposing parts of the substrates face each other and attains its minimum at $\delta = 0$. The force is maximal at $\delta/\zeta = 0.25$ and 0.75 where V_{lat} exhibits its strongest dependence on δ (Fig. 3). In Fig. 4 we show the decay of \mathcal{F}_{lat} as function of d . Asymptotically, $\mathcal{F}_{\text{lat}}/(k_B T S/\zeta^3)$ vanishes as $-0.003 e^{-2\pi d/\zeta}/(d/\zeta)$ for $\lambda_a/\zeta = 4$, $\lambda_b/\zeta = 8$, and $\delta/\zeta = 0.25$.

We note that due to the assumption $\zeta_a = \zeta_b$ interchanging λ_a and λ_b leaves the system unchanged [Fig. 1]. Thus the force must be identical for $\lambda_a \leftrightarrow \lambda_b$. While in Eqs. (20) and (21) this symmetry is explicitly valid up to the second order in $(\lambda_b - \lambda_a)$, the numerical results respect this symmetry fully. This provides a very useful check of the numerical calculations.

B. Lateral van der Waals force

Endowing the substrates with the envisaged stripe patterns requires corresponding chemical patterns which in

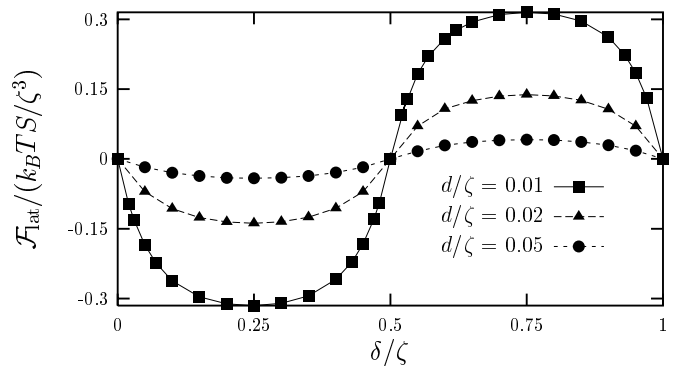


FIG. 2: The fluctuation-induced lateral force \mathcal{F}_{lat} in units of $k_B T S/\zeta^3$ between two periodically patterned substrates at distance d as function of the shift δ in units of the periodicity ζ for $d/\zeta = 0.01$, 0.02 , and 0.05 (see Fig. 1). The anchoring on the stripes in terms of the extrapolation lengths is taken to be $\lambda_a/\zeta = 4$ and $\lambda_b/\zeta = 8$. \mathcal{F}_{lat} is antisymmetric around $\delta/\zeta = 0.5$. There is no restoring force if the misalignment is maximal, i.e., at $\delta/\zeta = 0.5$. $\mathcal{F}_{\text{lat}} < 0$ means that the plates are pulled back towards the preferred alignment at $\delta = 0$; for $\mathcal{F} > 0$ the plates are pulled forward towards preferred alignment at $\delta = \zeta$.

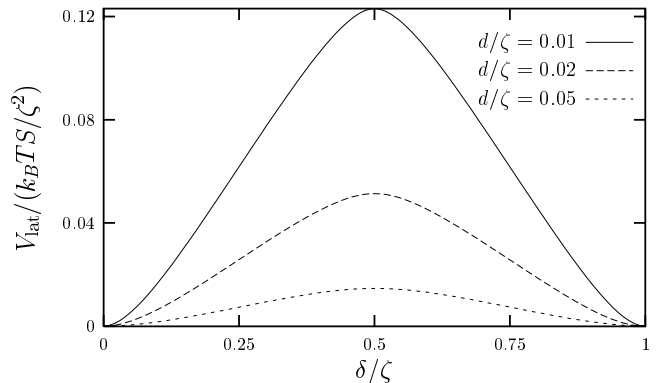


FIG. 3: The effective lateral potential $V_{\text{lat}}(\delta) = -\int_0^\delta \mathcal{F}_{\text{lat}}(\delta') d\delta'$ in units of $k_B T S/\zeta^2$ between two periodically patterned substrates at distance d as function of the shift δ in units of the periodicity ζ for $d/\zeta = 0.02$, 0.03 , and 0.05 and $\lambda_a/\zeta = 4$, $\lambda_b/\zeta = 8$. For all values of d/ζ the inflection points of the potential are at $\delta/\zeta = 0.25$ and 0.75 .

turn involve at least two different species providing the chemical contrast. These species do not only interact (differently) with the nematic liquid crystal in the vicinity of the substrate, giving rise to two different extrapolation lengths λ_a and λ_b , but also interact across the liquid crystal with each other via dispersion forces. The later interaction provides a lateral force as well which adds to the fluctuation-induced lateral force. Note that such a

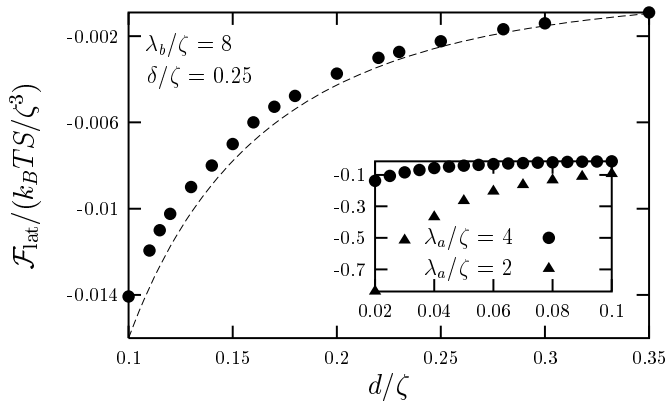


FIG. 4: The fluctuation-induced lateral force \mathcal{F}_{lat} in units of $k_B T S / \zeta^3$ between two periodically patterned substrates as function of the film thickness d in units of the periodicity ζ . The anchoring on the stripes in terms of the extrapolation lengths is taken to be $\lambda_a / \zeta = 4$, $\lambda_b / \zeta = 8$, and the lateral shift between the patterns is $\delta / \zeta = 0.25$. Asymptotically, $\mathcal{F}_{\text{lat}} / (k_B T S / \zeta^3)$ for $\delta / \zeta = 0.25$ vanishes as $-0.003 e^{-2\pi d / \zeta} / (d / \zeta)$ (dashed line). The variation of \mathcal{F}_{lat} for small values of d / ζ is shown in the inset for $\lambda_a / \zeta = 4$ (circles) and $\lambda_a / \zeta = 2$ (triangles). The other system parameters remain the same. As expected the absolute value of the amplitude of the lateral force increases upon increasing the contrast $|\lambda_b - \lambda_a|$.

lateral force due to direct interactions is the same if the two patterned substrates are separated by vacuum or by a nematic liquid crystal, as long as the *mean* nematic order is not affected by the stripe patterns.

In order to estimate these direct interactions between the patterned substrates, we consider each substrate to be covered by a monolayer whose chemical composition varies periodically, alternating between A- and B-particles. We neglect non-additivity aspects of the dispersion forces and consider pairwise interactions between the patterned monolayers at $z = 0$ and $z = d$. Since we consider d to be large compared with the diameters of the A and B particles, we can disregard that particles forming the monolayers occupy discrete lattice sites. As pair potentials between the two species we take Lennard-Jones potentials

$$u_{ij}(r) = 4\epsilon_{ij} \left[\left(\frac{\sigma_{ij}}{r} \right)^{12} - \left(\frac{\sigma_{ij}}{r} \right)^6 \right], \quad i, j = A, B \quad (22)$$

where A(B)-particles give rise to the extrapolation length $\lambda_{a(b)}$. Since in the present context $d \gg \sigma_{ij}$, for the lateral force only the attractive part of the pair potentials mat-

ters. This leads to the following expression for the van der Waals potential energy between the two monolayers:

$$V_{\text{lat}}^{\text{vdW}}(\delta) = - \int_S d^2 \mathbf{x}_1 \int_S d^2 \mathbf{x}_2 \frac{E(x_1, x_2; \delta)}{[d^2 + (\mathbf{x}_1 - \mathbf{x}_2)^2]^{3/2}} \quad (23)$$

with

$$E(x_1, x_2; \delta) = E_{AA} a(x_1) b(x_2; \delta) + E_{BA} [a(x_1) - 2a(x_1) b(x_2; \delta) + b(x_2; \delta)] + E_{BB} [1 - a(x_1)][1 - b(x_2; \delta)] \quad (24)$$

and

$$E_{ij} = 4\epsilon_{ij} \sigma_{ij}^6 \Sigma_i \Sigma_j \quad (25)$$

where $\Sigma_{A(B)}$ is the areal number density of A(B)-particles in the monolayer forming the stripe $\lambda_{a(b)}$. Carrying out the integration over y_1 and y_2 in Eq. (23), one obtains

$$V_{\text{lat}}^{\text{vdW}}(\delta) = - \frac{3\pi L}{8} \int_{-L/2}^{L/2} dx_1 \int_{-L/2}^{L/2} dx_2 \times \frac{E(x_1, x_2; \delta)}{[d^2 + (x_1 - x_2)^2]^{5/2}}, \quad (26)$$

where L is the lateral extension of the system both in the x and y directions. From this the lateral van der Waals force $\mathcal{F}_{\text{lat}}^{\text{vdW}} = -\partial_\delta V_{\text{lat}}^{\text{vdW}}(\delta)$ can be calculated:

$$\frac{\mathcal{F}_{\text{lat}}^{\text{vdW}}}{S} = \frac{E}{\zeta^5} f^{\text{vdW}}(\delta/\zeta, d/\zeta) \quad (27)$$

with the scaling function

$$f^{\text{vdW}}(\delta/\zeta, d/\zeta) = \frac{15\pi}{8} \sum_{n=-\infty}^{\infty} \int_{n+\delta/\zeta}^{n+1/2+\delta/\zeta} dX_1 \times \int_0^{1/2} dX_2 \frac{X_2 - X_1}{[(d/\zeta)^2 + (X_2 - X_1)^2]^{7/2}} \quad (28)$$

where $E = E_{AA} - 2E_{AB} + E_{BB}$. The force and the potential as function of δ/ζ are shown in Fig. 5. The comparison between Figs. 2 and 5 (a) reveals that the lateral van der Waals force is practically constant over a wide range of shift values and varies steeply around the positions of maximum and minimum misalignment while the fluctuation-induced force varies more smoothly across all shift values. Apart from that, the qualitative features are the same for both forces.

In order to estimate the lateral van der Waals force

we assume that the particles are closely packed within

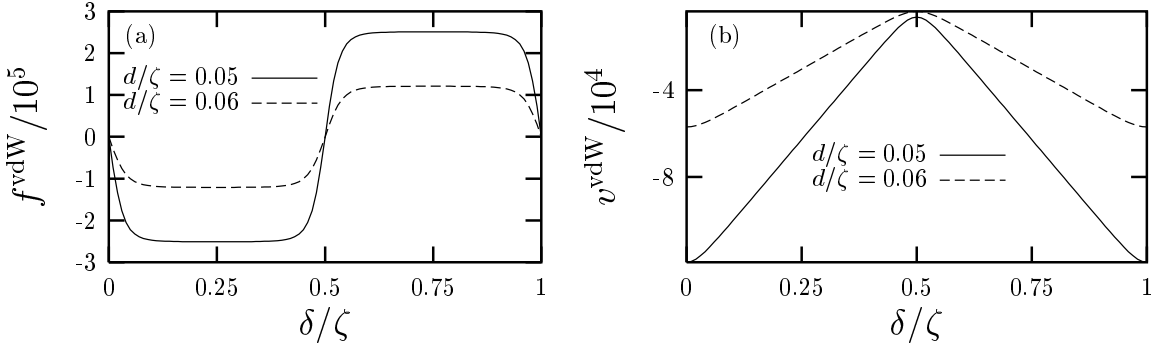


FIG. 5: (a) The dimensionless scaling function f^{vdW} [Eqs. (27) and (28)] of the lateral force induced by direct van der Waals interactions between the chemically patterned monolayers covering the two substrates at distance d as function of the shift δ in units of the periodicity ζ of the pattern for $d/\zeta = 0.05$ and 0.06 . (b) Corresponding lateral potential $V_{\text{lat}}^{\text{vdW}}(\delta) = \frac{ES}{\zeta^4} v_{\text{lat}}^{\text{vdW}}$ [Eq. (26)].

the monolayer [17], so that the areal number density is $\Sigma_{A(B)} = \sqrt{3}/(6R^2) \approx 2[\sigma_{AA(BB)}]^{-2}/\sqrt{3}$ where $R = \sigma_{AA}/2$ ($\sigma_{BB}/2$) is the radius of the A (B) particles forming a triangular lattice. According to Table I in Ref. [18] typical values are $\epsilon_{ij}/k_B \approx 300 K$ and $\sigma_{ij} \approx 0.5$ nm. For $\zeta = 200$ nm one has $E_{ij}/\zeta^5 \approx 1.5 \times 10^{-5}$ pN/ $(\mu\text{m})^2$. According to Fig. 5 (a) for $d/\zeta = 0.05$ this implies $\mathcal{F}_{\text{lat},ij}^{\text{vdW}} \approx 3$ pNS/ $(\mu\text{m})^2$ for the contribution $\propto E_{ij}$ to the actual lateral van der Waals force $\mathcal{F}_{\text{lat}}^{\text{vdW}}$ proportional to $E = E_{AA} - 2E_{AB} + E_{BB}$. Thus for a suitably chosen constant E , without compromising the goal of achieving $\lambda_a = \lambda_b/2$ (as used in our calculations), the lateral van der Waals force can be quite smaller than 3 pN per area $S/(\mu\text{m})^2$.

From Fig. 2 one finds, for the same system parameters ζ and d considered above and at room temperature, for the fluctuation-induced lateral force $\mathcal{F}_{\text{lat}} \approx 0.02$ pNS/ $(\mu\text{m})^2$. Thus the background lateral van der Waals force tends to be stronger than the nematic fluctuation induced force. However, for a suitably chosen chemical contrast of the particles forming the chemical stripes, it appears to be possible to determine the fluctuation-induced lateral force by measuring the shear force once with and once without the nematic liquid between the patterned substrates. The ratio of the two forces for $d/\zeta = 0.05$, $\lambda_a/\zeta = 4$, $\lambda_b/\zeta = 8$, and $E/\zeta^5 \approx 1.5 \times 10^{-5}$ pN/ $(\mu\text{m})^2$ as function of δ is shown in Fig. 6. It appears that the fluctuation-induced lateral force becomes more prominent around $\delta/\zeta = 0.25, 0.75$. From Figs. 2 and 5 (a) one notices that both $\mathcal{F}_{\text{lat}}/S$ and $\mathcal{F}_{\text{lat}}^{\text{vdW}}/S$ vanish linearly at $\delta/\zeta = 0, 0.5, 1.0$ [as $(-0.084 + 0.168 \delta/\zeta)$ pN/ $(\mu\text{m})^2$ and $(-33.5 + 66 \delta/\zeta)$ pN/ $(\mu\text{m})^2$ at $\delta/\zeta = 0.5$, respectively, for $d/\zeta = 0.05$, $E/\zeta^5 = 1.5 \times 10^{-5}$ pN/ $(\mu\text{m})^2$, $\zeta = 200$ nm, and $k_B T = 4 \times 10^{-21}$ J] and since the slope of $\mathcal{F}_{\text{lat}}^{\text{vdW}}$ is much larger than the corresponding slope of \mathcal{F}_{lat} , the ratio $\mathcal{F}_{\text{lat}}/\mathcal{F}_{\text{lat}}^{\text{vdW}}$ at $\delta/\zeta = 0, 0.5, 1.0$ is small. From Fig. 6 one should not draw the conclusion that the lateral fluctuation induced force is at most half a percent of the cor-

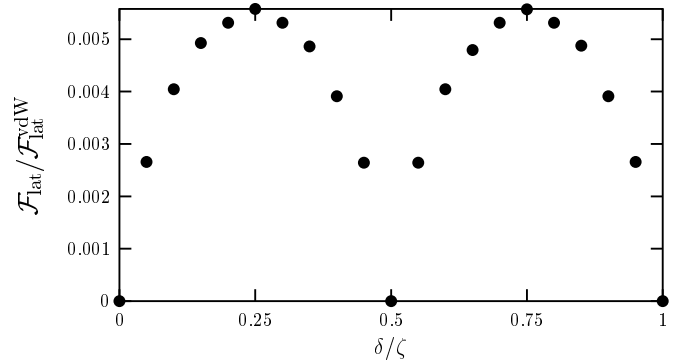


FIG. 6: The ratio of the fluctuation-induced lateral force \mathcal{F}_{lat} and the lateral van der Waals force $\mathcal{F}_{\text{lat}}^{\text{vdW}}$ as function of the shift δ in units of the periodicity ζ for $d/\zeta = 0.05$, $\lambda_a/\zeta = 4$, $\lambda_b/\zeta = 8$, $E/\zeta^5 \approx 1.5 \times 10^{-5}$ pN/ $(\mu\text{m})^2$, and at $T = 290$ K. \mathcal{F}_{lat} is more prominent around $\delta/\zeta = 0.25$ and 0.75 .

responding lateral van der Waals background force. This ratio is inversely proportional to $E = E_{AA} - 2E_{AB} + E_{BB}$. Figure 6 corresponds to a parameter choice for which E is estimated by an individual E_{ij} and not by the actual contrast expressed by E , which vanishes for $A = B$. Accordingly, for suitable choices of A and B , E can be significantly smaller than the E_{ij} used in Fig. 6 which then leads to a significantly larger ratio.

IV. FLUCTUATION-INDUCED NORMAL FORCE

The effect of a periodic anchoring at one substrate, with the second substrate being homogeneous, on the fluctuation-induced normal force was studied in Ref. [11]. It turned out that for the description of the normal force the single patterned substrate can be replaced by a uni-

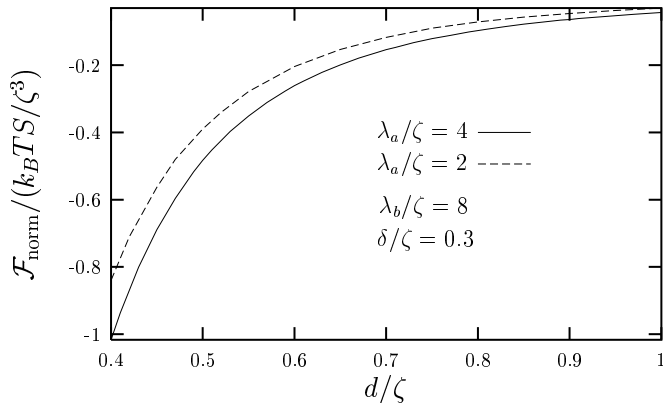


FIG. 7: The fluctuation-induced normal force $\mathcal{F}_{\text{norm}}$ in units of $k_B T S/\zeta^3$ between two periodically patterned substrates as function of the film thickness d in units of the periodicity ζ . The anchoring on the stripes in terms of the extrapolation lengths is taken to be $\lambda_b/\zeta = 8$ and $\lambda_a/\zeta = 4$ (full line), 2 (dashed line). For $d < \lambda_a, \lambda_b$ as shown here the anchoring is weak but finite [5] at both substrates and the force is attractive. As expected the absolute value of the amplitude of the force decreases upon decreasing the extrapolation length. The force depends very weakly on the shift δ . Here δ/ζ is set to 0.3.

form substrate with an effective anchoring strength, i.e., the force is given by the force found between two uniform substrates characterized by their effective anchoring. Depending on the model parameters, the normal force is either repulsive or attractive – corresponding to an effective similar-dissimilar or an effective similar-similar boundary condition, respectively. In the present case of two patterned substrates, we have calculated the normal force numerically [Eq. (16)]. Figure 7 shows the dependence of the normal force $\mathcal{F}_{\text{norm}}$ on d . For $d < \lambda_a, \lambda_b$ as shown here, the force is attractive and decays monotonically as function of d . In this regime, the anchoring is weak at both substrates so that the effect of the periodicity is not visible. We note that in this case the fluctuation-induced normal force [Fig. 7] is about 1000 (100) times larger than the fluctuation-induced lateral force [Fig. 4] for $\lambda_a/\zeta = 4$ (2). Figure 8, however, shows the behavior of $\mathcal{F}_{\text{norm}}$ as function of δ in the regime of strong but finite anchoring $d > \lambda_a, \lambda_b$. In this case the normal force is oscillatory and attractive, and its magnitude is comparable with the fluctuation-induced lateral force [Fig. 9].

V. SUMMARY AND CONCLUSION

We have calculated the fluctuation-induced forces acting on two substrates chemically modulated with period

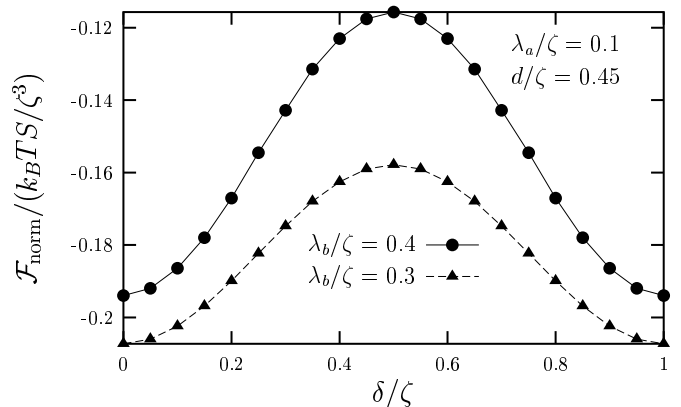


FIG. 8: The fluctuation-induced normal force $\mathcal{F}_{\text{norm}}$ in units of $k_B T S/\zeta^3$ between two periodically patterned substrates at distance $d/\zeta = 0.45$ as function of the shift δ in units of the periodicity ζ . The anchoring on the stripes in terms of the extrapolation lengths is taken to be $\lambda_a/\zeta = 0.1$ and $\lambda_b/\zeta = 0.3$ (triangles), 0.4 (circles). For $d > \lambda_a, \lambda_b$ as shown here the anchoring is strong but finite at both substrates and the force is attractive. As expected the absolute value of the amplitude of the force decreases upon increasing the extrapolation length [5]. The force oscillates as function of the shift δ and for complete misalignment, i.e., $\delta/\zeta = 0.5$ the attraction is weakest.

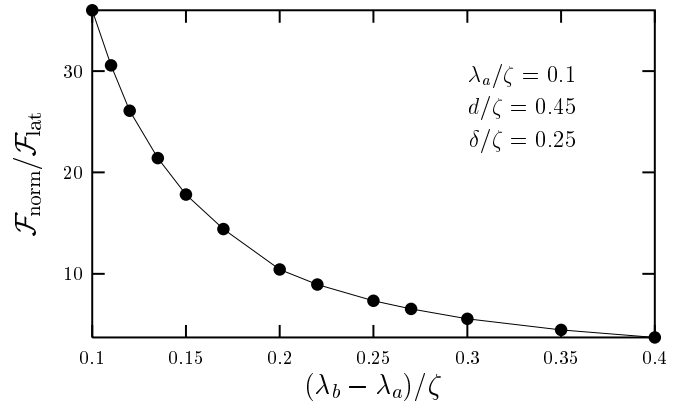


FIG. 9: Fluctuation-induced normal force $\mathcal{F}_{\text{norm}}$ divided by fluctuation-induced lateral force \mathcal{F}_{lat} as function of the contrast $\lambda_b - \lambda_a$ in units of the periodicity ζ for $\lambda_a/\zeta = 0.1$, $d/\zeta = 0.45$, corresponding to strong but finite anchoring, and $\delta/\zeta = 0.25$. $\mathcal{F}_{\text{norm}}$ and \mathcal{F}_{lat} are of comparable size.

ζ and confining a nematic film of thickness d (Fig. 1). The substrates are characterized by homeotropic anchoring with alternating extrapolation lengths λ_a and λ_b . We have studied the shear force as function of the lateral shift δ between the patterns on the substrates and of their separation d . For $|\lambda_b - \lambda_a| \ll \lambda_a$ and $\zeta \ll d$, the lateral force sinusoidally oscillates as a function of

δ/ζ and decays exponentially with d/ζ [Eq. (20) and Fig. 4]. For stronger contrasts, the lateral force and its corresponding potential have been evaluated numerically [Figs. 2 and 3]. It turns out that for a suitably chosen chemical contrast the fluctuation-induced lateral force is comparable [Fig. 6] with the background lateral van der Waals force between the corresponding monolayers on the top and bottom substrates forming the chemical heterogeneity [Fig. 5]. In order to complete the picture of the forces in the presence of the patterned substrates we have also calculated numerically the fluctuation-induced normal forces [Figs. 7 and 8] and found them to be comparable with the fluctuation-induced lateral force in the case of strong anchoring [Fig. 9].

Patterning at small length scales gives rise to rich interfacial phenomena. Surface modulations open the possibility of controlling the morphology of wetting films and generate structural phase transitions which are central to the behavior of structural forces induced by distortions of the liquid crystal order parameter. In such cases, in addition to the fluctuation-induced forces, the substrates are subject to liquid-crystalline *elastic* forces [3]. Such elastic forces scale with K [Eq. (2)] and are for large d larger than the fluctuation-induced forces which scale with $k_B T$. Since for small d the elastic forces scale as $d^{-0.5}$ [2] but

the fluctuation-induced force as d^{-3} [5], the latter can, however, even dominate for small d . The *mean field* director contributions are completely eliminated for such model parameters and boundary conditions for which the director structure is uniform. In Ref. [19] it has been demonstrated that this uniformity can indeed occur for suitable combinations of model parameters, even in cases of competing planar and homeotropic anchoring conditions, which have not been considered here. Capillary forces due to capillary condensation and the formation of bridge phases [20, 21, 22] are other sources for the structural forces in the vicinity of the nematic-isotropic phase transition. If the fluid is confined to very narrow slits, patterning may give rise to capillary bridges of different liquid crystalline order. Under such conditions, it would be interesting to study the stress under the shear strains by shifting the lateral substrate structures out of phase [23] which might give rise to rather strong lateral forces.

Lateral forces can technologically be used to align the parallel substrate structures. For instance, for those ranges of the model parameters for which the liquid crystalline lateral forces are significant, the liquid crystal can be filled into the slit pore to align the substrate structure and then be removed.

-
- [1] P. G. de Gennes and J. Prost, *The Physics of Liquid Crystals* (Clarendon, Oxford, 1993).
- [2] S. Kondrat, A. Poniewierski, and L. Harnau, *Eur. Phys. J. E* **10**, 163 (2003).
- [3] A. Poniewierski and S. Kondrat, *J. Mol. Liq.* **112**, 61 (2004).
- [4] A. Ajdari, L. Peliti, and J. Prost, *Phys. Rev. Lett.* **66**, 1481 (1991).
- [5] P. Zihrel, R. Podgornik, and S. Žumer, *Chem. Phys. Lett.* **295**, 99 (1998).
- [6] P. Zihrel, F. Karimi Pour Haddadan, R. Podgornik, and S. Žumer, *Phys. Rev. E* **61**, 5361 (2000).
- [7] F. Karimi Pour Haddadan, D. W. Allender, and S. Žumer, *Phys. Rev. E* **64**, 061701 (2001).
- [8] P. Zihrel and I. Mušević, *Liq. Cryst.* **28**, 1057 (2001).
- [9] T. Emig, A. Hanke, R. Golestanian, and M. Kardar, *Phys. Rev. A* **67**, 022114 (2003).
- [10] R. Büscher and T. Emig, preprint, cond-mat/0412766 (2004).
- [11] F. Karimi, F. Schlesener, and S. Dietrich, *Phys. Rev. E* **70**, 041701 (2004).
- [12] H. Li and M. Kardar, *Phys. Rev. Lett.* **67**, 3275 (1991).
- [13] R. Golestanian and M. Kardar, *Phys. Rev. A* **58**, 1713 (1998).
- [14] T. Emig, *Europhys. Lett.* **62**, 466 (2003).
- [15] R. Büscher and T. Emig, *Phys. Rev. A* **69**, 062101 (2004).
- [16] A. Hanke, private communication.
- [17] P. M. Chaikin and T. C. Lubensky, *Principles of condensed matter physics* (Cambridge University Press, Cambridge, 1995).
- [18] T. Getta and S. Dietrich, *Phys. Rev. E* **47**, 1856 (1993).
- [19] S. Kondrat, A. Poniewierski, and L. Harnau, *Liq. Cryst.* **32**, 95 (2005).
- [20] K. Kočevar, A. Borštnik, I. Mušević, and S. Žumer, *Phys. Rev. Lett.* **86**, 5914, (2001).
- [21] D. Andrienko, P. Patrício, and O. I. Vinogradova, *J. Chem. Phys.* **121**, 4414 (2004).
- [22] H. Stark, J.-I. Fukuda, and H. Yokoyama, *Phys. Rev. Lett.* **92**, 205502 (2004).
- [23] H. Bock and M. Schoen, *J. Phys: Condens. Matter* **12**, 1545 (2000).